ルスしか含まないような検体は，検査で確実に陽性となることはない．しかし，400 mL採血由来のFFPは約240 mLの容量があり，10単位の濃厚血小板にも約200 mLの血漿が含まれている．厚生労働省の「血液製剤等に係る遡及調査ガイドライン」や日本輸血・細胞治療学会の「輸血療法の実施に関する指針」では，輸血実施患者について肝炎ウイルスおよびHIVに対する感染リスクを考慮し，ウイルス関連マーカーの検査実施を求めている．また，輸血後肝炎が疑われHAV，HBV，HCVが否定された場合は，HEV感染も考慮して原因調査を行うことが必要である．

文　献

1) 片山　透：輸血後感染症に関する研究，厚生省血液研究事業．平成17年度研究報告集．

2) 日本赤十字社：輸血情報 0811-116（日本赤十字社 HP）．

3) Takahashi K, et al: Full-genome nucleotide sequence of a hepatitis E virus strain that may be indigenous to Japan. Virology **287**: 9-12, 2001.

4) Tei S, et al: Zoonotic transmission of hepatitis E virus from deer to human beings. Lancet **362**: 371-373, 2003.

5) Matsubayashi K, et al: Transfusion-transmitted hepatitis E caused by apparently indigenous hepatitis E virus strain in Hokkaido, Japan. Transfusion **44**: 934-940, 2004.

6) Goeland P, et al: Molecular and serologic tracing of a transfusion-transmitted hepatitis A virus. Transfusion **44**: 1555-1561, 2004.

7) Hughes JA, et al: Case report of a transfusion-associated hepatitis A infection. Transfusion **54**: 2202-2206, 2014.

8) Tabuchi A, et al: Titration of hepatitis B virus infectivity in the sera of pre-acute and late acute phases of HBV infection: Transmission experiments to chimeric mice with human liver repopulated hepatocytes. J Med Virol **80**: 2064-2068, 2008.

9) Koyama Y, et al: Minimum infectious dose of hepatitis B virus in chimpanzees and difference in the dynamics of viremia between genotype A and genotype C. Transfusion **48**: 286-294, 2008.

10) Glynn SA, et al: Dynamics of viremia in early hepatitis C virus infection. Transfusion **45**: 994-1002, 2005.

11) Busch MP, et al: Infectivity in chimpanzees (*Pan troglodytes*) of plasma collected before HCV RNA detectability by FDA-licensed assays: implications for transfusion safety and HCV infection outcomes. Blood **119**: 6326-6334, 2012.

12) Schüttler CG, et al: Hepatitis C virus transmission by a blood donation negative in nucleic acid amplification tests for viral RNA. Lancet **355**: 41-42, 2000.

13) Katayama K, et al: Titration of hepatitis C virus in chimpanzees for determining the copy number required for transmission. Intervirology **47**: 57-64, 2004.

14) Sakata H, et al: A nationwide survey for hepatitis E virus prevalence in Japanese blood donors with elevated alanine aminotransferase. Transfusion **48**: 2568-2576, 2008.

15) 川村欣也ほか：静岡県西部地区で発生したシカ生肉またはイノシシ生肝摂食後のE型急性肝炎3例．肝臓 **51**: 418-424, 2010.

ORIGINAL ARTICLE

Branched-chain amino acids reduce hepatic iron accumulation and oxidative stress in hepatitis C virus polyprotein-expressing mice

Masaaki Korenaga[1,2], Sohji Nishina[1], Keiko Korenaga[1], Yasuyuki Tomiyama[1], Naoko Yoshioka[1], Yuichi Hara[1], Yusuke Sasaki[3], Yasushi Shimonaka[3] and Keisuke Hino[1]

1 Department of Hepatology and Pancreatology, Kawasaki Medical School, Okayama, Japan
2 The Research Center for Hepatitis and Immunology, National Center for Global Health and Medicine (NCGM), Chiba, Japan
3 Product Research Department, Chugai Pharmaceutical Co., Kanagawa, Japan

Abstract

Background & Aims: Branched-chain amino acids (BCAA) reduce the incidence of hepatocellular carcinoma (HCC) in patients with cirrhosis. However, the mechanisms that underlie these effects remain unknown. Previously, we reported that oxidative stress in male transgenic mice that expressed hepatitis C virus polyprotein (HCVTgM) caused hepatic iron accumulation by reducing hepcidin transcription, thereby leading to HCC development. This study investigated whether long-term treatment with BCAA reduced hepatic iron accumulation and oxidative stress in iron-overloaded HCVTgM and in patients with HCV-related advanced fibrosis. *Methods:* Male HCVTgM were fed an excess-iron diet that comprised either casein or 3.0% BCAA, or a control diet, for 6 months. *Results:* For HCVTgM, BCAA supplementation increased the serum hepcidin-25 levels and antioxidant status [ratio of biological antioxidant potential (BAP) relative to derivatives of reactive oxygen metabolites (dROM)], decreased the hepatic iron contents, attenuated reactive oxygen species generation, and restored mitochondrial superoxide dismutase expression and mitochondrial complex I activity in the liver compared with mice fed the control diet. After 48 weeks of BCAA supplementation in patients with HCV-related advanced fibrosis, BAP/dROM and serum hepcidin-25 increased and serum ferritin decreased compared with the pretreatment levels. *Conclusions:* BCAA supplementation reduced oxidative stress by restoring mitochondrial function and improved iron metabolism by increasing hepcidin-25 in both iron-overloaded HCVTgM and patients with HCV-related advanced fibrosis. These activities of BCAA may partially account for their inhibitory effects on HCC development in cirrhosis patients.

Hepatitis C virus (HCV) causes acute and chronic hepatitis, cirrhosis, and hepatocellular carcinoma (HCC) (1). New direct-acting antiviral treatments are expected to eliminate this virus in about 90% of patients (2), but therapies that could reduce disease progression in chronically infected individuals would be highly beneficial.

Valine, leucine and isoleucine are essential branched-chain amino acids (BCAA). A decreased ratio of serum

BCAA relative to aromatic amino acids, a hallmark of cirrhosis, is caused by several factors, including reduced nutritional intake and ammonia detoxification in skeletal muscles (3). BCAA supplementation can improve the nutritional status and albumin synthesis by activating the mammalian target of rapamycin signalling cascade (4, 5) and glucose metabolism in skeletal muscles (6, 7). Long-term oral BCAA supplementation decreases the frequency of HCC in male obese patients with cirrhosis (8). BCAA also had an antihepatocarcinogenic activity in an animal model of insulin resistance (9, 10). In addition, glucose intolerance is closely linked to hepatocarcinogenesis. However, the mechanisms that underlie these effects remain unknown.

Hepatic oxidative stress and iron overload have been implicated in liver injury and hepatocarcinogenesis in HCV-associated chronic liver diseases (11, 12). The HCV core protein inhibits mitochondrial complex I and generates reactive oxygen species (ROS) in vivo (13). Previously, we reported that HCV-induced ROS increases the hepatic iron concentration by reducing hepcidin transcription in transgenic mice that express HCV polyprotein (14), where even modest iron supplementation in these mice resulted in the development of liver tumours, including HCC, because of mitochondrial injury (15). Thus, hepatic iron overload and oxidative stress via mitochondrial injury are critical during HCC pathogenesis.

In the present study, we examined whether long-term BCAA supplementation could prevent the development of hepatic iron accumulation and oxidative stress in HCV transgenic mice fed an excess-iron diet and in patients with HCV-related advanced fibrosis.

Materials and methods

Animals and experimental design

The pAlbSVPA-HCV transgene contains the full-length HCV polyprotein-coding region under the control of the murine albumin promoter/enhancer (16, 17). HCV polyprotein is processed into individual proteins in the liver and expressed at biologically relevant levels in FL-N/35 transgenic mice (HCVTgM) (17). In the present study, male HCVTgM (8 weeks old) were fed a normal rodent diet, including carbonyl iron (45 mg/kg; control, $n = 6$), or an excess-iron diet (carbonyl iron, 225 mg/kg) that contained either 3.0% BCAA (BCAA/iron; $n = 5$) or casein (casein/iron; $n = 7$). Six months later, the mice were sacrificed by CO_2 asphyxiation after a 12-h fast, according to the criteria outlined in the Guide for the Care and Use of Laboratory Animals.

Clinical chemistry tests

The serum concentrations of alanine aminotransferase, aspartate aminotransferase (AST), albumin, glucose, insulin, BCAA, tyrosine and hepcidin-25 were determined in blood samples collected from the inferior vena cava of sacrificed mice at 12 h after fasting. The blood glucose levels were periodically measured using a glucometer (OneTouch Ultra, Lifescan, Inc., Milpitas, CA, USA). The serum insulin levels were measured using an ultrasensitive mouse insulin ELISA kit (Morinaga Milk, Kanagawa, Japan). The serum hepcidin-25 levels were determined by LC/MS/MS (18).

Hepatic iron and triglyceride contents

The hepatic iron concentrations were measured by atomic absorption spectrometry, as described previously (15). The liver tissue was homogenized and the lipids were extracted (19), and the triglyceride levels were measured using a TGE-test Wako kit (Wako Pure Chemicals, Tokyo, Japan), according to the manufacturer's instructions. The protein concentrations were determined by the Lowry method (20) using a DC protein assay kit (Bio-Rad Laboratories, Hercules, CA, USA).

In situ ROS detection

In situ liver ROS production was assessed by staining with dihydroethidium (Invitrogen Corp., Carlsbad, CA, USA), as described previously (14). Dihydroethidium is oxidized to ethidium bromide in the presence of ROS, which stains the nuclei bright red via DNA intercalation (21). The intensity of the fluorescence was quantified using the NIH Image analysis program in three randomly selected areas of the digital images for each mouse.

Derivatives of reactive oxygen metabolites and biological antioxidant potential levels

The derivatives of reactive oxygen metabolites (dROM) and biological antioxidant potential (BAP) levels were measured using a Free Radical Elective Evaluator (Wismerll Co. Ltd, Tokyo, Japan) (22, 23). The dROM measurements were determined based on the ability of transition metals to catalyse the formation of coloured free radicals (detection at 505 nm). The results were expressed in Cartelli units (U.CARR), where 1 U.CARR = 0.8 mg/L of H_2O_2. To obtain the BAP measurements, the blood samples were added to a solution containing $FeCl_3$ bound to a chromogenic substrate (AT, a derivative of thiocyanate). Fe^{3+} reduction to Fe^{2+} caused a chromatic change that was directly proportional to the plasma ROS reduction, which was measured at 505 nm using a photometer. Blood aliquots (10 μl) were mixed with the $FeCl_3$ solution and incubated for 5 min at 37°C before the photometric analysis.

Histological staining

Part of each liver sample was snap-frozen immediately in liquid nitrogen to determine the hepatic triglycerides

and iron concentration. The remaining liver tissue was fixed in 4% paraformaldehyde in phosphate-buffered saline and embedded in paraffin for use in the histological analysis. The liver sections were stained with haematoxylin and eosin.

Real-time reverse transcriptase-PCR

One-step real-time real-time reverse transcriptase-PCR (RT-PCR) was performed, as described previously (14), where the results were expressed as the hepcidin, interleukin 6 (IL6), BMP6 and superoxide dismutase 2 (SOD2) gene mRNA levels relative to β-actin mRNA.

Extraction of nuclear and histone deacetylase activity assay

For isolation of nuclear proteins from mice liver, Nuclear Extraction Kit 1 (Epigentek, Farmingdale, NY, USA) was used. Histone deacetylase (HDAC) activity was assessed using HDAC Activity/Inhibition Direct Assay Kit (Epigentek) according to the manufacturer's instruction.

Isolation of mitochondria and complex I activity determination

Liver mitochondria were isolated and the activity of complex I was assayed (at 25°C) as described previously (3, 24).

Protein extraction and Western blotting

The liver lysate and mitochondrial lysate proteins were separated by sodium dodecyl sulphate-polyacrylamide gel electrophoresis. These proteins were then transferred to polyvinylidene difluoride membranes (Millipore, Bedford, MA, USA) and blocked overnight at 4°C with 1–3% skim milk and 0.1% Tween 20 in Tris-buffered saline, which was followed by incubation at room temperature for 1 h with a primary antibody. Anti-rabbit carnitine palmitoyl transferase I (CPT I), anti-rabbit CPT II (Alpha Diagnostic International, San Antonio, TX, USA), anti-rabbit SREBP1 (Santa Cruz Biotechnology Inc., Santa Cruz, CA, USA), or anti-bacterially expressed mouse CCAAT/enhancer-binding protein homology protein (CHOP) fusion protein (Abcam, Cambridge, England) were used for the liver lysate proteins. Anti-SOD2 (Abcam), anti-Grp75 (mitochondrial heat shock protein70; Abcam), or anti-NDUFB8 (mitochondrial complex I) antibody (Abcam) were used for the mitochondrial lysates. The proteins were blocked for 1 h at room temperature and then incubated overnight at 4°C with a Phospho-stat3 (pSTAT3) antibody (Cell Signaling Technology Inc., Danvers, MA, USA) and a Phospho-Smad1/Smad5/Smad8 (pSMAD1/5/8) antibody (Cell Signaling Technology Inc.).The anti-acetyl-

histoneH3K9 and anti-histoneH3 (Cell Signaling Technology Inc,) were used for the nuclear lysates.

Human BCAA supplementation study design

We screened 68 HCV RNA-positive patients who were aged >65 years (Fig. S1). We enrolled 25 patients with HCV-related advanced fibrosis who satisfied the following criteria: serum albumin = 3.5–4.2 g/dl; platelet counts <15 × 10^4/μl; amino acid imbalance [based on the ratio of BCAA relative to tyrosine (BTR) <4.40, which was lower than the normal limits]; and no HCC or symptoms of chronic liver failure such as ascites, varices or hepatic encephalopathy. Advanced fibrosis defined liver specimens (METAVIR fibrosis staging: >F3,4) or Fib-4 index (>3.25). The patients were assigned randomly to receive BCAA supplementation (BCAA group; $n = 12$) or follow-up without treatment (non-BCAA group; $n = 13$). BCAA group were given a 4 g BCAA preparation (LIVACT Granules; Ajinomoto, Tokyo, Japan) administered orally three times daily after meals. We measured the plasma oxidized/reduced albumin and serum dROM and BAP as oxidative stress markers at 12, 24 and 48 weeks after starting the treatment. We also measured the levels of serum iron, ferritin, transferrin saturation (TSAT) and hepcidin-25 to evaluate the oxidative stress-associated iron metabolism. Moreover, type IV collagen 7s, type III procollagen peptide (PIIP) and Fib-4 index were measured to confirm the degree of hepatic fibrosis.

Written informed consent was obtained from each study participant. This study was conducted in accordance with the provisions of the 1975 Declaration of Helsinki and it was approved by the Institutional Ethics Committee of Kawasaki Medical School.

Statistical analysis

The results were expressed as mean ± SD. The group results were compared using Levene's or Welch's tests. The changes in the levels of the iron metabolism and oxidative stress markers between the BCAA and the non-BCAA groups were analysed using Wilcoxon rank-sum tests. Pearson's product moment correlation coefficient was used to assess associations between the dihydroethidium-positive areas and the BAP and dROM ratios. Differences were considered statistically significant at $P < 0.05$. The statistical analyses were performed using SPSS software (IBM SPSS Statistics 20.0 for Windows).

Results

AST, fasting blood sugar, plasma BCAA and tyrosine levels in HCVTgM

The dietary intake and body weight did not differ significantly between the three groups of mice. BCAA administration for 6 months significantly reduced the serum

AST ($P < 0.05$) and fasting blood sugar (FBS) levels ($P < 0.05$) compared with HCV TgM fed the excess-iron diet with casein (casein/iron group) (Table 1). However, the FBS levels remained higher in the HCVTgM fed the excess-iron diet with BCAA (BCAA/iron group) compared with the HCV TgM fed a normal rodent diet (control group) ($P < 0.05$). The casein/iron group had significantly lower plasma BCAA and the ratio of BCAA relative to tyrosine (BTR) levels ($P < 0.05$) compared with the BCAA/iron and control groups (Table 1). The tyrosine levels were significantly higher in the casein/iron group than the control group ($P < 0.05$).

Hepatic iron contents and hepcidin-25 levels in HCVTgM

The hepatic iron contents of HCVTgM fed the excess-iron diet with casein were significantly higher than those of HCVTgM fed an excess-iron diet with BCAA or a control diet at 6 months after the treatment commenced (Fig. 1A). The hepcidin levels of HCVTgM fed the excess-iron diet with BCAA were significantly higher than those of HCVTgM fed the excess-iron diet with casein or the control diet (Fig. 1A). The serum hepcidin to ferritin ratio was lower in patients with HCV (25). The serum hepcidin-25 to hepatic iron ratio was significantly higher in HCVTgM fed the excess-iron diet with BCAA compared with those fed the excess-iron diet with casein or the control diet.

ROS generation

BCAA administration resulted in significantly lower dROM levels and an increased BAP to dROM ratio (BAP/dROM) compared with casein administration ($P < 0.05$; Fig. 1B). Hepatic ROS production, which

was determined by dihydroethidium staining, was significantly higher in HCVTgM fed the excess-iron diet with casein compared with those fed the excess-iron diet with BCAA or the control diet (Fig. 1C). The BAP/dROM ratios were negatively correlated with hepatic ROS production in all mice ($r = 0.8985$; $n = 15$; $P < 0.01$; Fig. 1D).

Factors that affected hepcidin upregulation

HCV-induced ROS production downregulates hepcidin transcription by inhibiting the C/EBPα DNA-binding activity of CHOP (14). Thus, we examined CHOP expression and the hepcidin mRNA levels. Hepatic CHOP expression was significantly lower and hepatic hepcidin expression was significantly higher in HCVTgM fed the excess-iron diet with BCAA compared with the levels in HCVTgM fed the excess-iron diet plus casein (Fig. 2A,B). The IL-6-gp130/signal transducer and activator of transcription are involved in the regulation of hepcidin transcription (26). Another pathway that regulates hepcidin expression involves the TGF-β/ bone morphogenetic protein superfamily (27, 28). Thus, we examined the STAT-IL6 and SMAD-BMP signalling pathways. There were no differences in the phosphate STAT3, IL6, phosphor- SMAD1/5/8 and BMP6 expression levels between the BCAA and casein groups (Fig. 2C). In addition, HCV-induced oxidative stress inhibited hepcidin expression through increased histone deacetylase (HDAC) activity in cell culture system (29). HDAC activity of HCV TgM fed the excess-iron diet with BCAA was significantly lower than those of HCVTgM fed the excess-iron diet with casein or the control diet (Fig. S2). These results suggested that BCAA induced the upregulation of hepatic hepcidin by enhancing the antioxidant potential.

Hepatic steatosis and CPT1 expression

HCVTgM fed the excess-iron diet developed severe steatosis, including the centrilobular microvesicular type (15, 17). Previous studies showed that the antioxidant drugs N-acetylcysteine (NAC) and Stronger Neo-Minophagen C (SNMC) reduce the hepatic triglyceride levels in a dose-dependent manner (30, 31). In the present study, BCAA administration tended to reduce the hepatic triglyceride levels ($P = 0.055$; Fig. 3A).

Thus, we examined the effects of BCAA on CPT1 and CPT2, which are proteins that regulate long-chain fatty acid oxidation in mitochondria, and SREBP1 expression, which is a transcription factor that activates genes required for lipogenesis. Our previous study indicated that decreased CPT1 and increased SREBP1 expression contribute to the development of hepatic steatosis in HCVTgM fed an excess-iron diet (30). In the present study, CPT1 expression increased significantly in HCVTgM fed the excess-iron diet with BCAA after 6 months ($P < 0.05$, Fig. 3C), whereas CPT2 expression

Table 1. Effects of casein/iron and branched-chain amino acids (BCAA)/iron diets on the liver to body weight ratios and blood chemistry results in hepatitis C virus transgenic mice
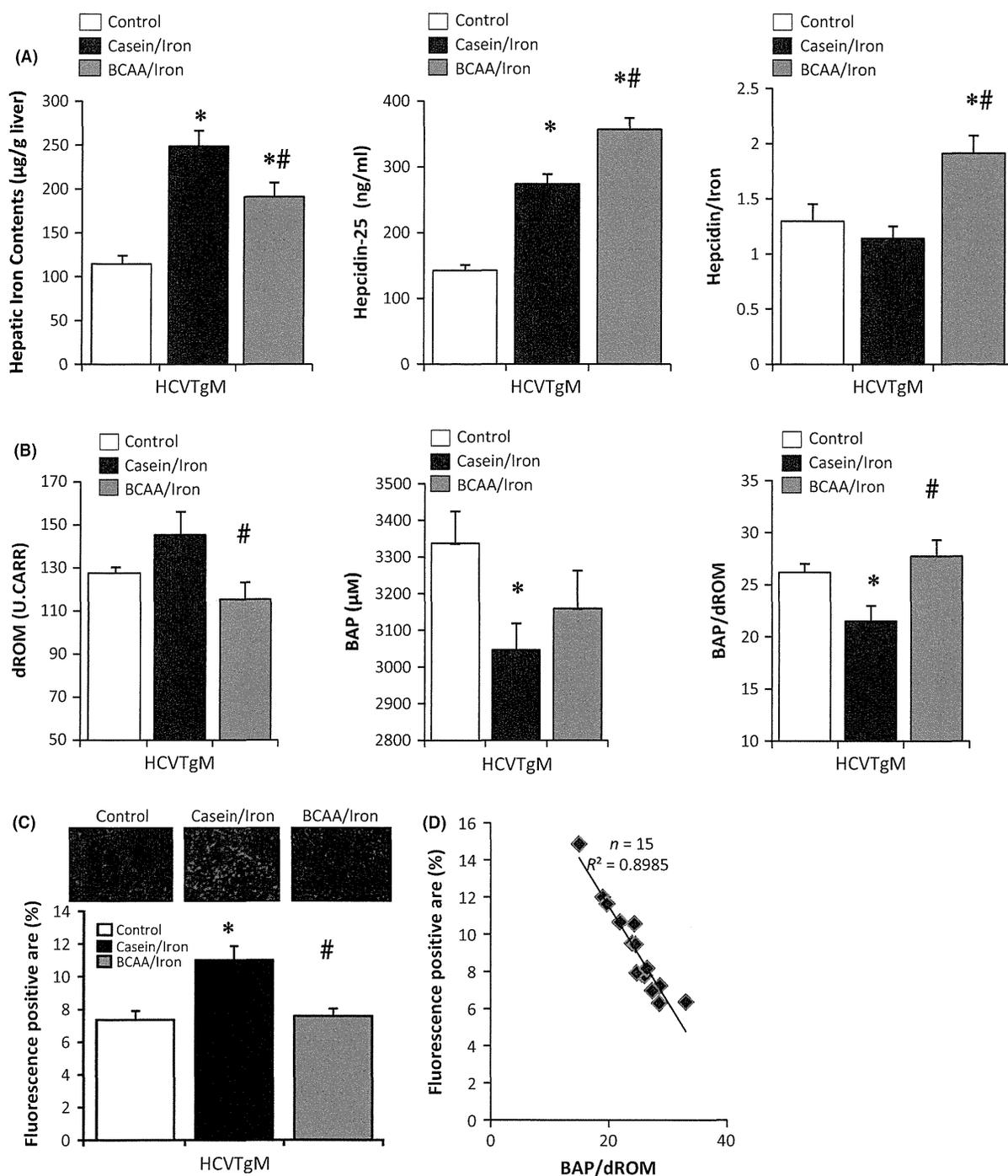
	Control	Casein/iron	BCAA/iron
Mice (*N*)	6	7	5
Liver weight/ Body weight (%)	3.32 ± 0.30	3.50 ± 0.60	2.97 ± 0.28
AST (IU/L)	61 ± 23	92 ± 47	39 ± 7‡
ALT (IU/L)	14 ± 4	61 ± 60	16 ± 4
FBS (mg/dl)	115 ± 11	299 ± 49†	184 ± 47†‡
Insulin (ng/ml)	0.89 ± 0.36	1.19 ± 0.20	0.93 ± 0.39
Albumin (g/dl)	2.82 ± 0.04	2.77 ± 0.15	2.96 ± 0.15
BCAA (nmol/ml)	313 ± 22	275 ± 31†	318 ± 35‡
Tyrosine (nmol/ml)	63 ± 5	82 ± 11†	69 ± 11
BTR	5.01 ± 0.20	3.41 ± 0.40†	4.67 ± 0.40‡

*Results are mean ± SD.

†$P < 0.05$ vs. transgenic mice expressing hepatitis C virus polyprotein (HCVTgM) on control diet for 6 months.

‡$P < 0.05$ vs. HCVTgM on excess-iron diet with casein for 6 months.

ALT, alanine aminotransferase; AST, aspartate aminotransferase; FBS, fasting blood sugar.

Fig. 1. (A) Hepatic iron contents, hepcidin-25 levels, and hepcidin-25 to iron content ratios (hepcidin/iron). (Left) Hepatic iron contents in mice at 6 months after starting treatment for the control (n = 6), casein/iron (n = 7) and BCAA/iron groups (n = 5). (Centre) Serum hepcidin-25 levels. (Right) The hepcidin/iron ratios were used as an index of the sensitivity of hepcidin upregulation against iron overload. (B) Oxidative stress markers in serum. (Left) dROM and (centre) BAP were measured at 6 months after starting treatment. (Right) The antioxidant status was determined as the BAP to dROM ratio. (C) Dihydroethidium fluorescence intensity was quantified for three randomly selected areas in digital images for the control (n = 3), casein/iron (n = 7), and BCAA/iron groups (n = 5) at 6 months after starting treatment. (D) Correlations between the BAP/dROM ratios and fluorescence-positive areas in liver. *P < 0.05 vs control group; #P < 0.05 vs casein/iron group.
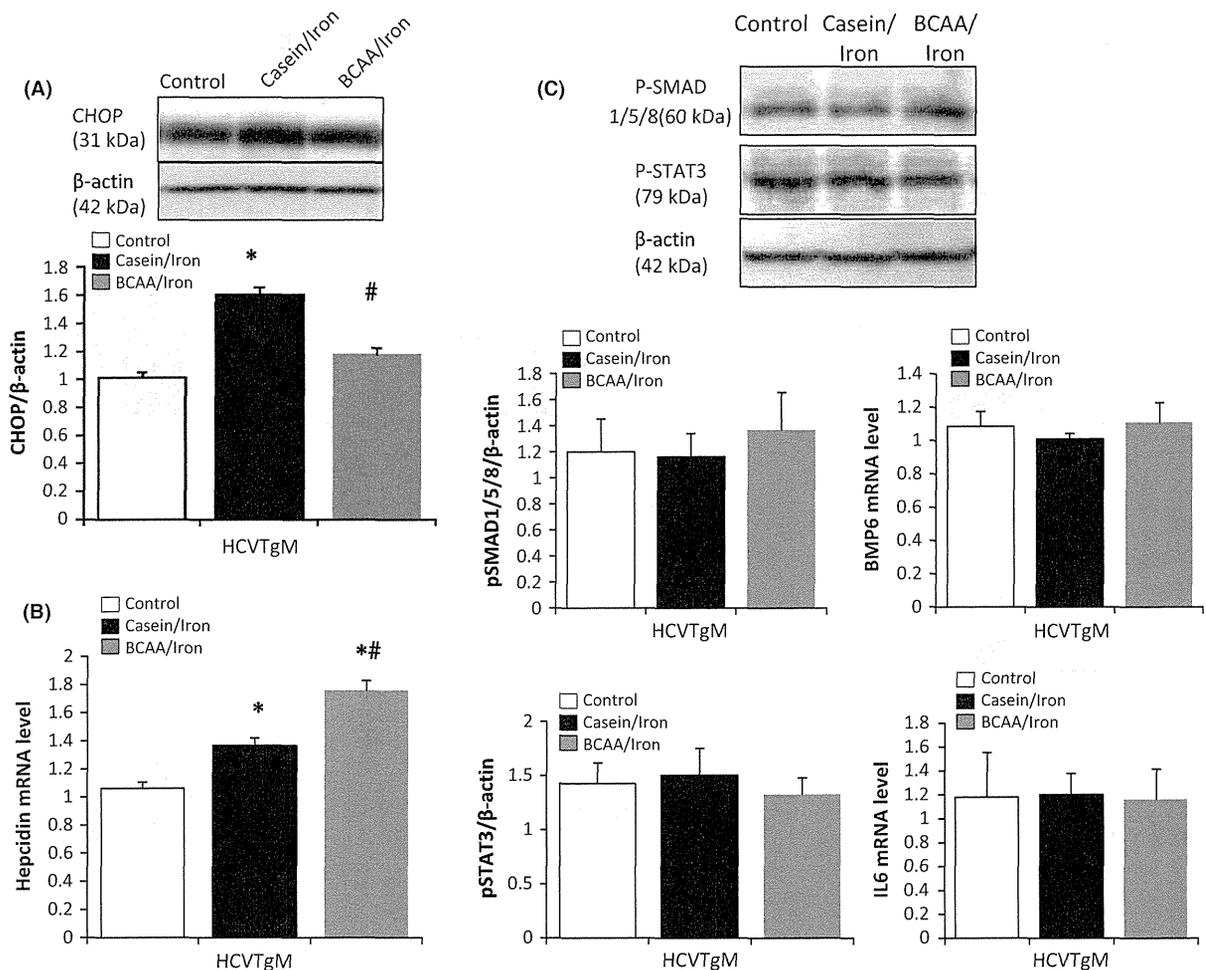
Fig. 2. (A) Immunoblots for CHOP after 6 months of treatment. (B) Liver hepcidin expression was determined for four mice in each group (C) Immunoblots for p-SMAD1/5/8 and (C) p-STAT3 after 6 months of treatment. (C) BMP6and (C) IL6 mRNA expression was determined for four mice in each group. The protein expression levels were normalized against that of β-actin. *$P < 0.05$ vs control group; #$P < 0.05$ vs casein/iron group.

did not increase significantly. However, SREBP1 expression did not decrease in HCVTgM fed the excess-iron diet with BCAA ($P = 0.082$; Fig. 3B). These results suggest that the administration of BCAA was insufficient to prevent iron-induced steatosis in HCVTgM because BCAA failed to reduce SREBP1 expression.

SOD2 expression and mitochondrial complex I activity

CPT1 is localized to the mitochondrial outer membrane. Decreased CPT1 expression may be related to the HCV core protein's association with the mitochondrial outer membrane. The HCV core protein interacts with mitochondria complex I, which generates ROS (13). Alterations in the mitochondrial ultrastructure were observed in HCVTgM fed the excess-iron diet after 6 months, as described previously (15, 30). We exam-

ined whether BCAA supplementation reduced iron- and HCV-induced mitochondrial injury.

The mitochondrial SOD2 mRNA levels were significantly higher in HCVTgM fed the excess-iron diet with BCAA compared with those fed the excess-iron diet with casein or the control diet. The SOD2 expression levels in mice fed the excess-iron diet with casein were significantly lower than those fed the control diet. However, the SOD2 expression levels were restored by BCAA supplementation (Fig. 4A). After 6 months, the mitochondrial complex I expression levels were significantly lower in mice fed the excess-iron diet with casein compared with those fed the control diet. Similar to SOD2, the mitochondrial complex I expression levels were restored by BCAA supplementation (Fig. 4B).

The enzymatic activity of mitochondrial complex I was significantly lower in mice fed the excess-iron diet
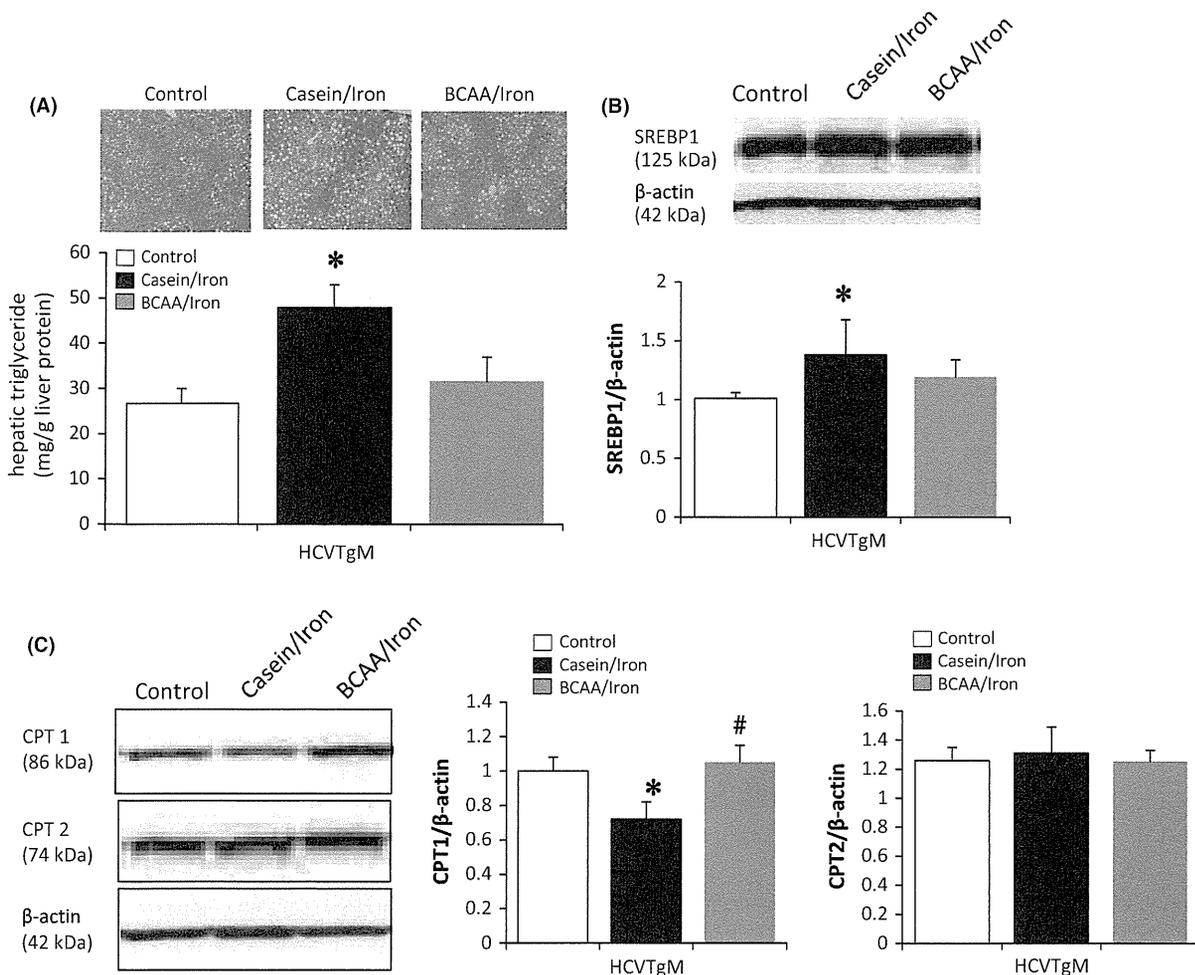
Fig. 3. (A) Hepatic steatosis in HCVTgM fed the excess-iron diet with BCAA and HCVTgM fed the excess-iron diet with casein after treatment for 6 months (haematoxylin and eosin, original magnification × 100). The hepatic triglyceride levels were determined. (B) Immunoblots of SREBP1, (C) CPT1, and (C) CPT2 in the livers of three mice from each group. *$P < 0.05$ vs control group; #$P < 0.05$ vs casein/iron group.

with casein compared with those fed the control diet. The activity was restored by BCAA supplementation (Fig. 4C). Thus, these improvements in the mitochondrial complex I activity and CPT1, SOD2, and mitochondrial complex I expression indicate that BCAA may protect against the mitochondrial injury induced by HCV proteins and iron overload.

Antioxidant effects of BCAA supplementation in patients with HCV-related severe fibrosis

Next, we determined whether oral BCAA supplementation reduced oxidative stress and affected iron metabolism in patients with HCV-related advanced liver fibrosis. We assigned 25 patients to receive either BCAA supplementation (BCAA group; $n = 12$) or follow-up without treatment (non-BCAA group; $n = 13$). There were no differences in the clinical characteristics, oxidative stress

markers, or iron metabolic markers at baseline between these groups (Table 2). Serum albumin and AST levels in BCAA group tended to be lower than those in non-BCAA group, although these differences were not statistically significant ($P = 0.071$ and $P = 0.074$ respectively).

The dROM levels increased significantly at weeks 24 and 48 in the non-BCAA group, whereas they did not in the BCAA group. The BAP levels also increased at weeks 12 and 24 in the non-BCAA group, and at weeks 12, 24 and 48 in the BCAA group (Table 3). The BAP/dROM ratio, an indicator of antioxidant potential, decreased significantly at week 48 in the non-BCAA group, but increased at weeks 24 and 48 in the BCAA group. This suggests that the BAP levels of the non-BCAA group increased in response to oxidative stress, while the increased BAP levels in the BCAA group indicated enhanced antioxidant potential.
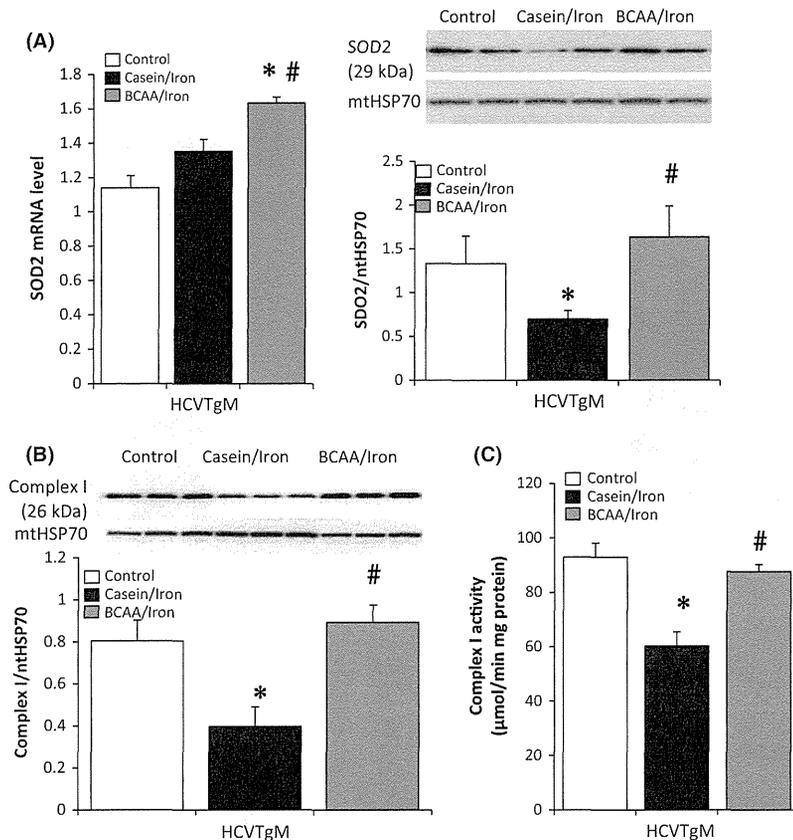
Fig. 4. (A) SOD2 mRNA expression in the livers of four mice from each group. (B) Immunoblots of SOD2 and mitochondrial complex I in the mitochondria of four mice from each group after treatment for 6 months. The protein expression levels were normalized against that of mitochondrial heat shock protein 70. *P < 0.05 vs control group; #P < 0.05 vs casein/iron group.

In agreement with the antioxidant status, the serum ferritin levels were significantly lower after week 48 of BCAA supplementation (137 ± 109 mg/dl; P < 0.05) compared with those before treatment (Table 3). BCAA supplementation significantly increased the serum hepcidin-25 levels at week 48 (20.2 ± 14.5 mg/dl; P < 0.05). In addition, we determined the level of albumin synthesis after BCAA supplementation, because the oxidized albumin to total albumin ratio increases with cirrhosis progression and it is related to oxidative stress (32,33). In the present study, there were no differences in the total albumin changes in the non-BCAA or BCAA groups (Table 4). However, the amount of albumin present in the reduced form increased significantly in the BCAA group at week 48 compared with that before the study. By contrast, the level of reduced albumin decreased significantly at week 48 in the non-BCAA group. This suggests that long-term BCAA supplementation reduced iron overload by upregulating antioxidant potential and this improved the albumin status in patients without hypoalbuminaemia and chronic liver failure.

Discussion

Hepatic iron overload and ROS production are both pathophysiological features of HCV-associated chronic liver disease (34) and risk factors for HCC development (35). The reduced hepatic oxidative stress observed after oral BCAA supplementation may be related to changes in the albumin redox state (32, 36). However, previous studies did not determine how BCAA affects iron metabolism and ROS generation.

The mouse model used in the present study shared similarities with the patients who had HCV-associated chronic liver disease in terms of hepatic ROS production and steatosis (14) at 6 months after treatment, followed by hepatocarcinogenesis (15). Furthermore, the hepatic iron concentrations in HCVTgM fed the excess-iron diet were comparable to those of a large number of patients with chronic hepatitis C (30, 37, 38). Thus, HCVTgM fed the excess-iron diet is a suitable model for assessing the effects of long-term supplementation with BCAA on disordered iron metabolism and ROS production in HCV infection.

Table 2. Patient baseline characteristics

	non-BCAA	BCAA	*P*-value
Patients (*N*)	13	12	N.S.
Age (years)	73.5 (65–87)	74.9 (65–83)	N.S.
Sex (male/female)	6/7	6/6	N.S.
White blood cell count ($\times 10^2/mm^3$)	46.2 (30.1–63.4)	45.1 (27.1–84.5)	N.S.
Haemoglobin concentration (g/dl)	13.3 (10.6–16.3)	13.2 (11.4–15.7)	N.S.
Platelet counts ($\times 10^4/mm^3$)	12.2 (4.9–15)	10.5 (3.7–15)	N.S.
Total bilirubin (mg/dl)	0.7 (0.5–1.1)	1.0 (0.3–1.7)	N.S.
Albumin (g/dl)	4.0 (3.5–4.2)	3.9 (3.5–4.2)	N.S.
ALT (IU/L)	33 (23–47)	41 (21–55)	N.S.
AST (IU/L)	43 (32–54)	48 (32–54)	N.S.
ALP (IU/L)	286 (158–435)	302 (145–491)	N.S.
GTP (IU/L)	46 (15–177)	53 (16–137)	N.S.
FBS (mg/dl)	94 (70–130)	107 (72–158)	N.S.
Insulin (μIU/ml)	14 (5.3–39)	14 (6.3–28)	N.S.
Tyrosine (nmol/ml)	104 (76–123)	103 (63–149)	N.S.
BCAA (nmol/ml)	424 (319–606)	401 (269–617)	N.S.
BTR	4.1 (2.6–4.9)	4.0 (2.7–4.4)	N.S.
AFP (ng/dl)	11 (2–61)	18 (2–95)	N.S.
Serum iron (μg/ml)	134 (50–255)	136 (37–256)	N.S.
TSAT (%)	38 (11–70)	44 (12–88)	N.S.
Ferritin (ng/ml)	120 (30–429)	190 (30–346)	N.S.

Results are mean (range). Comparisons between branched-chain amino acids (BCAA) and non-BCAA groups were made using Levene's or Welch's tests. AFP, α-foetoprotein; ALP, alkaline phosphatase; ALT, alanine aminotransferase; AST, aspartate aminotransferase; GGT, gamma glutamyltransferase; BTR, the ratio of BCAA relative to tyrosine; FBS, fasting blood sugar; N.S., Not significant; TSAT, transferrin saturation.

BCAA supplementation improves the nutritional status, prognosis and quality of life for patients with cirrhosis (39, 40). A randomized, controlled trial demonstrated that BCAA supplementation reduced the frequency of HCC in obese male patients with cirrhosis and HCV infection (18). BCAA treatment also reduced the hepatocarcinogenic activity in obese diabetic animals with insulin resistance (9, 10). Insulin resistance promotes hepatocarcinogenesis by activating the mitogen-activated protein kinase (MAPK) pathway and insulin-like growth factor 1 (IGF-1) receptors, which further activates the Raf/MAPK kinase/MAPK cascade (41, 42). BCAA suppress the IGF/IGF-1R axis by down-regulating IGF-1, IGF-2 and IGF-1R mRNA expression, thereby leading to the inhibition of mitosis and cell growth (9). BCAA reduce HCC development by inhibiting insulin resistance (43).

In the present study, the FBS levels of HCVTgM fed the excess-iron diet with casein increased after 6 months. BCAA supplementation reduced the iron overload-induced elevation of the FBS. There was no intrahepatic inflation or fibrosis in the HCVTgM fed the excess-iron diet, but those fed the excess-iron diet with casein had significantly lower plasma BCAA levels and a lower BTR compared with those fed excess-iron with BCAA and the control diet. An amino acid imbalance, which is indicated by a lower BTR, has been observed in patients with compensated cirrhosis or chronic hepatitis (44, 45). This suggests that BCAA might potentially reduce hepatic iron accumulation and ROS in patients with HCV-related advanced fibrosis.

Table 3. Changes in oxidative stress and iron metabolism markers during branched-chain amino acids (BCAA) administration*

	Week 0	Week 12	Week 24	Week 48
Hepcidin (ng/ml)				
non-BCAA	11.6 ± 7.9	10.4 ± 9.8	11.8 ± 9.5	10.5 ± 8.8
BCAA	9.5 ± 8.7	9.2 ± 9.5	11.0 ± 9.1	20.2 ± 14.5†
Ferritin (ng/ml)				
non-BCAA	120 ± 121	112 ± 105	100 ± 108	118 ± 120
BCAA	190 ± 135	164 ± 129	163 ± 130	137 ± 109†
Serum iron (μg/ml)				
non-BCAA	134 ± 52	143 ± 60	133 ± 55	142 ± 38
BCAA	136 ± 64	131 ± 63	134 ± 68	117 ± 57
TSAT (%)				
non-BCAA	38 ± 14	42 ± 19	39 ± 15	42 ± 19
BCAA dROM (U.CARR)	45 ± 29	42 ± 24	35 ± 19†	33 ± 16†
non-BCAA	342 ± 64	405 ± 84	431 ± 76†	455 ± 96†
BCAA	360 ± 113	372 ± 80	361 ± 118	359 ± 65
BAP (uM)				
non-BCAA	2369 ± 386	2772 ± 487†	2798 ± 337†	2630 ± 64
BCAA	2139 ± 587	2516 ± 678†	2601 ± 647†	2758 ± 413†
BAP/dROM				
non-BCAA	7.0 ± 1.0	7.1 ± 1.7	6.6 ± 0.7	6.0 ± 1.0†
BCAA	6.1 ± 1.3	6.8 ± 1.5	7.5 ± 1.6†	7.8 ± 1.5†

*Results are mean ± SD.
†$P < 0.05$ vs. before BCAA treatment, Wilcoxon rank-sum test; U.CARR, Cartelli Units (1 U.CARR = 0.8 mg/L of H_2O_2), TSAT, transferrin saturation.

Table 4. Changes in the serum albumin characteristics during branched-chain amino acid (BCAA) administration*

	Week 0	Week 12	Week 24	Week 48
Albumin (g/dl)				
non-BCAA (13)	4.0 ± 0.2	4.0 ± 0.2	4.0 ± 0.2	4.0 ± 0.2
BCAA (12)	3.9 ± 0.3	3.8 ± 0.4	3.9 ± 0.3	4.0 ± 0.3
Reduced albumin (%)				
non-BCAA (10)	66 ± 4.5	66 ± 5.3	66 ± 3.9	63 ± 4.9†
BCAA (10)	66 ± 3.9	68 ± 2.8	68 ± 5.2	70 ± 3.2†
Type IV collagen 7s (U/ml)				
non-BCAA (13)	5.8 ± 1.7	6.1 ± 2.5	6.0 ± 2.2	6.1 ± 2.1
BCAA (12)	6.8 ± 2.1	7.1 ± 1.8	7.0 ± 2.1	6.7 ± 2.0
P-III-P (U/ml)				
non-BCAA (13)	0.89 ± 0.19	0.83 ± 0.19	0.91 ± 0.24	0.83 ± 0.15
BCAA (12)	0.88 ± 0.23	0.90 ± 0.16	0.88 ± 0.18	0.86 ± 0.22
Fib4-index				
non-BCAA (13)	5.0 ± 2.7	5.0 ± 2.5	5.4 ± 2.9	5.5 ± 3.7
BCAA (12)	6.8 ± 4.2	7.2 ± 3.7	6.4 ± 4.0	6.3 ± 4.0

*Results are mean ± SD.

†$P < 0.05$ vs. before treatment, Wilcoxon rank-sum test, P-III-P: Type III procollagen peptide.

Our previous study indicated that the antioxidant N-acetylcysteine (NAC) almost completely blocked ROS production and abrogated the hepatic steatosis induced by HCV proteins and iron (30). In the present study, the hepatic triglyceride levels tended to be lower in mice fed the excess-iron diet with BCAA compared with those fed the excess-iron diet with casein, although these differences were not statistically significant ($P = 0.055$). This may have been because BCAA reduce ROS production to a lesser degree than NAC, or because BCAA supplementation did not completely inhibit the ROS-associated unfolded protein response or improve glucose intolerance compared with the control diet. SREBP1 expression is positively regulated by insulin signalling pathways (46). Therefore, further studies are needed to determine whether BCAA reduce hepatic iron accumulation without affecting hepatic steatosis.

CPT1, a transmembrane enzyme in the mitochondrial outer membrane, is negatively regulated at the transcriptional level by malonyl-CoA, which is an intermediate product of fatty acid synthesis (47). Decreased CPT1 expression may be related to the HCV core protein, which is also located in the mitochondrial outer membrane and it generates mitochondrial ROS production indirectly (13). BCAA enhanced protection against mitochondrial injury by restoring the mitochondrial antioxidant potential and mitochondrial complex I activity. Thus, how does BCAA protect from HCV-induced ROS production and mitochondrial injury? The hepatic ROS production increased more in the HCVTgM fed the control diet compared with non-transgenic mice (14), but we did not test whether BCAA supplements reduced ROS production in HCVTgM without the excess-iron diet. However, there were no differences in the liver enzyme, glucose, insulin, BCAA and tyrosine levels of HCVTgM and non-transgenic mice. Furthermore, HCVTgM without the excess-iron

diet did not develop severe steatosis and HCC. This indicates that HCVTgM without the excess-iron diet are not a suitable model for long-term treatments with BCAA.

BCAA supplementation increases the reduced form of albumin, which is a predictor of the cirrhosis prognosis (32, 33), while it also improves oxidative stress and iron metabolism in patients with decompensated cirrhosis (36), and in rats exposed to a fibrogenic agent (48). This suggests that the antioxidant effects of BCAA may be related to qualitative changes in serum albumin or the upregulation of albumin synthesis (4, 5, 9, 49). BCAA itself activates the mammalian target of rapamycin, which subsequently upregulates the downstream molecules, eukaryotic initiation factor 4E-binding protein-1 and 70-kDa ribosomal protein S6 kinase, thereby regulating mRNA translation and synthesis (50). In the present clinical study, we confirmed that long-term BCAA supplementation increased the BAP/dROM ratios and serum hepcidin-25 levels, whereas it decreased the serum ferritin levels in patients with HCV-related advanced fibrosis. Moreover, we found that BAP continued to increase from week 12 to week 48, and the level of the reduced albumin form increased at week 48, but without changes in the serum albumin levels, in our BCAA group. The mechanism that allows BCAA to protect against HCV and iron-induced oxidative stress remains uncertain, but BCAA may improve iron metabolism by upregulating the antioxidant potential in patients without decompensated cirrhosis.

In addition, amino acid imbalance is a risk factor for HCC development in patients without hypoalbuminaemia (40), which suggests that BCAA supplementation should be recommended to patients with amino acid imbalances with advanced fibrosis, who may have a decreased antioxidant potential and reduced albumin level. In this study, we could not show any effect by

which BCAA supplementation prevented fibrotic progression (Table 4). However, Fib-4 index in BCAA group at 48 weeks tended to be decreased compared with those at initial point, although these differences were not statistically significant ($P = 0.061$). Long-term BCAAs treatment might inhibit hepatic fibrosis in HCV patients with advanced fibrosis.

Our clinical study had some limitations, including a higher number of older patients who had higher serum albumin and ferritin levels than those in the cohorts reported in other studies, although they used small sample sizes and were not randomized. Further studies should use large cohorts to clarify these effects.

In conclusion, we demonstrated that BCAA administration reduced the hepatic iron contents and ROS levels, which were induced by HCV proteins and iron overloading in mice, probably by protecting the function of mitochondrial complex I. Furthermore, we confirmed that BCAA supplementation improved disordered iron metabolism and the antioxidant status in patients with HCV-related advanced fibrosis. These effects of BCAA may partially account for their inhibitory effects on HCC development in patients with cirrhosis.

Acknowledgements

References

1. Seeff LB. Natural history of chronic hepatitis C. *Hepatology* 2002; **36**: S35–46.
2. Lawitz E, Mangia A, Wyles D, *et al.* Sofosbuvir for previously untreated chronic hepatitis C infection. *N Engl J Med* 2013b; **368**(20): 1878–87.
3. Yamato M, Muto Y, Yoshida T, Kato M, Moriwaki H. Clearance rate of plasma branched-chain amino acids correlates significantly with blood ammonia level in patients with liver cirrhosis. *Int Hepatol Commun* 1995; **3**: 91–6.
4. Nishitani S, Ijichi C, Takehana K, Fujitani S, Sonaka I. Pharmacological activities of branched-chain amino acids: specificity of tissue and signal transduction. *Biochem Biophys Res Commun* 2004; **313**: 387–9.
5. Kuwahata M, Yoshimura T, Sawai Y, *et al.* Localization of polypyrimidine-tract-binding protein is involved in the regulation of albumin synthesis by branched-chain amino acids in HepG2 cells. *J Nutr Biochem* 2008; **19**: 438–47.
6. Nishitani S, Matsumura T, Fujitani S, *et al.* Leucine promotes glucose uptake in skeletal muscles of rats. *Biochem Biophys Res Commun* 2002; **299**: 693–6.
7. She P, Reid TM, Bronson SK, *et al.* Disruption of BCATm in mice leads to increased energy expenditure associated with the activation of a futile protein turnover cycle. *Cell Metab* 2007; **6**: 181–94.
8. Muto Y, Sato S, Watanabe A, *et al.* Overweight and obesity increase the risk for liver cancer in patients with liver cirrhosis and long-term oral supplementation with branched chain amino acid granules inhibits liver carcinogenesis in heavier patients with liver cirrhosis. *Hepatol Res* 2006; **35**: 204–14.
9. Iwasa J, Shimizu M, Shiraki M, *et al.* Dietary supplementation with branched-chain amino acids suppresses diethylnitrosamine-induced liver tumorigenesis in obese and diabetic C57BL/KsJ-db/db mice. *Cancer Sci* 2010; **101**: 460–7.
10. Yoshiji H, Noguchi R, Kaji K, *et al.* Attenuation of insulin-resistance-based hepatocarcinogenesis and angiogenesis by combined treatment with branched-chain amino acids and angiotensin-converting enzyme inhibitor in obese diabetic rats. *J Gastroenterol* 2010; **45**: 443–50.
11. Farinati F, Cardin R, De Maria N, *et al.* Iron storage, lipid peroxidation and glutathione turnover in chronic anti-HCV positive hepatitis. *J Hepatol* 1995; **22**: 449–56.
12. Kato J, Kobune M, Nakamura T, *et al.* Normalization of elevated hepatic 8-hydroxy-2'-deoxyguanosine levels in chronic hepatitis C patients by phlebotomy and low iron diet. *Cancer Res* 2001; **61**: 8697–702.
13. Korenaga M, Wang T, Li Y, *et al.* Hepatitis C virus core protein inhibits mitochondrial electron transport and increases reactive oxygen species (ROS) production. *J Biol Chem* 2005; **280**: 37481–8.
14. Nishina S, Hino K, Korenaga M, *et al.* Hepatitis C virus-induced reactive oxygen species raise hepatic iron level in mice by reducing hepcidin transcription. *Gastroenterology* 2008; **134**: 226–38.
15. Furutani T, Hino K, Okuda M, *et al.* Hepatic iron overload induces hepatocellular carcinoma in transgenic mice expressing the hepatitis C virus polyprotein. *Gastroenterology* 2006; **130**: 2087–98.
16. Beard MR, Abell G, Honda M, *et al.* An infectious molecular clone of a Japanese genotype 1b hepatitis C virus. *Hepatology* 1999; **30**: 316–24.
17. Lerat H, Honda M, Beard MR, *et al.* Steatosis and liver cancer in transgenic mice expressing the structural and nonstructural proteins of hepatitis C virus. *Gastroenterology* 2002; **122**: 352–65.
18. Murao N, Ishigai M, Yasuno H, Shimonaka Y, Aso Y. Simple and sensitive quantification of bioactive peptides in biological matrices using liquid chromatography/selected reaction monitoring mass spectrometry coupled with trichloroacetic acid clean-up. *Rapid Commun Mass Spectrom* 2007; **21**: 4033–8.
19. Bligh EG, Dyer WJ. A rapid method of total lipid extraction and purification. *Can J Biochem Physiol* 1959; **37**: 911–7.
20. Lowry OH, Rosebrough NJ, Farr AL, Randall RJ. Protein measurement with the Folin phenol reagent. *J Biol Chem* 1951; **193**: 265–75.
21. Harrison-Findik DD, Schafer D, Klein E, *et al.* Alcohol metabolism-mediated oxidative stress down-regulates hep-

cidin transcription and leads to increased duodenal iron transporter expression. *J Biol Chem* 2006; **281**: 22974–82.

22. Cesarone MR, Belcaro G, Carratelli M, *et al.* A simple test to monitor oxidative stress. *Int Ang* 1999; **2**: 127–30.

23. Dohi K, Satoh K, Nakamachi T, *et al.* Does edaravone (MCI-186) act as an antioxidant and neuroprotector in experimental traumatic brain injury? *Antioxid Redox Signal* 2007; **8**: 281–7.

24. Jarreta D, Orus J, Barrientos A, *et al.* Mitochondrial function in heart muscle from patients with idiopathic dilated cardiomyopathy. *Cardiovasc Res* 2000; **45**: 860–5.

25. Fujita N, Sugimoto R, Motonishi S, *et al.* Patients with chronic hepatitis C achieving a sustained virological response to peginterferon and ribavirin therapy recover from impaired hepcidin secretion. *J Hepatol* 2008; **49**: 702–10.

26. Pietrangelo A, Dierssen U, Valli L, *et al.* STAT3 is required for IL-6-gp130-dependent activation of hepcidin in vivo. *Gastroenterology* 2007; **132**: 294–300.

27. Wang RH, Li C, Xu X, *et al.* A role of SMAD4 in iron metabolism through the positive regulation of hepcidin expression. *Cell Metab* 2005; **2**: 399–409.

28. Babitt JL, Huang FW, Wrighting DM, *et al.* Bone morphogenetic protein signaling by hemojuvelin regulates hepcidin expression. *Nat Genet* 2006; **38**: 531–9.

29. Miura K, Taura K, Kodama Y, Schnable B, Brenner DA. Hepatitis C virus–induced oxidative stress suppresses hepcidin expression through increase histone deacetylase activity. *Hepatology* 2008; **48**: 1420–9.

30. Nishina S, Korenaga M, Hino K, *et al.* Hepatitis C virus protein and iron overload induce hepatic steatosis through the unfolded protein response in mice. *Liver Int* 2010; **30**: 683–92.

31. Korenaga M, Hidaka I, Nishina S, *et al.* A glycyrrhizin-containing preparation reduces hepatic steatosis induced by hepatitis C virus protein and iron overload in mice. *Liver Int* 2011; **31**: 552–60.

32. Fukushima H, Miwa Y, Shiraki M, *et al.* Oral branched-chain amino acid supplementation improves the oxidized/reduced albumin ratio in patients with liver cirrhosis. *Hepatol Res* 2007; **37**: 765–70.

33. Oettl K, Birner-Gruenberger R, Spindelboeck W, *et al.* Oxidative albumin damage in chronic liver failure: relation to albumin binding capacity, liver dysfunction and survival. *J Hepatol* 2013; **59**: 978–83.

34. Kitase A, Hino K, Furutani T, *et al.* In situ detection of oxidized n-3 polyunsaturated fatty acids in chronic hepatitis C: correlation with hepatic steatosis. *J Gastroenterol* 2005; **40**: 617–24.

35. Kato J, Miyanishi K, Kobune M, *et al.* Long-term phlebotomy with low-iron diet therapy lowers risk of development of hepatocellular carcinoma from chronic hepatitis C. *J Gastroenterol* 2007; **42**: 830–6.

36. Ohno T, Tanaka Y, Sugauchi F, *et al.* Suppressive effect of oral administration of branched-chain amino acid granules on oxidative stress and inflammation in HCV-positive patients with liver cirrhosis. *Hepatol Res* 2008; **38**: 683–8.

37. Hofer H, Osterreicher C, Jessner W, *et al.* Hepatic iron concentration does not predict response to standard and pegylated-IFN/ribavirin therapy in patients with chronic hepatitis C. *J Hepatol* 2004; **40**: 1018–22.

38. Rulyak SJ, Eng SC, Patel K, *et al.* Relationships between hepatic iron content and virologic response in chronic hepatitis C patients treated with interferon and ribavirin. *Am J Gastroenterol* 2005; **100**: 332–7.

39. Kawaguchi T, Izumi N, Charton MR, Sata M. Branched-chain amino acids as pharmacological nutrients in chronic liver disease. *Hepatology* 2011; **54**: 1063–70.

40. Kawaguchi T, Shiraishi K, Ito T, *et al.* Branched-chain amino acids prevent hepatocarcinogenesis and prolong survival of patients with cirrhosis. *Clin Gastroenterol Hepatol* 2014; **12**: 1012-8.e1.

41. Formisano P, Oriente F, Fiory F, *et al.* Insulin-activated protein kinase C beta bypasses Ras and stimulates mitogen-activated protein kinase activity and cell proliferation in muscle cells. *Mol Cell Biol* 2000; **20**: 6323–33.

42. Sandhu MS, Dunger DB, Giovannucci EL. Insulin, insulin-like growth factor-I (IGF-I), IGF binding proteins, their biologic interactions, and colorectal cancer. *J Natl Cancer Inst* 2002; **94**: 972–80.

43. Kawaguchi T, Nagao Y, Matsuoka H, Ide T, Sata M. Branched-chain amino acid-enriched supplementation improves insulin resistance in patients with chronic liver disease. *Int J Mol Med* 2008; **22**: 105–12.

44. Suzuki K, Suzuki K, Koizumi K, *et al.* Measurement of serum branched-chain amino acids to tyrosine ratio level is useful in a prediction of a change of serum albumin level in chronic liver disease. *Hepatol Res* 2008; **38**: 267–72.

45. Michitaka K, Hiraoka A, Kume M, *et al.* Amino acid imbalance in patients with chronic liver diseases. *Hepatol Res* 2010; **40**: 393–8.

46. Kohjima M, Higuchi N, Kato M, *et al.* SREBP-1c, regulated by the insulin and AMPK signaling pathways, plays a role in nonalcoholic fatty liver disease. *Int J Mol Med* 2008; **21**: 507–11.

47. Kerner J, Hoppel C. Fatty acid import into mitochondria. *Biochim Biophys Acta* 2000; **1486**: 1–17.

48. Iwasa M, Kobayashi Y, Mifuji-Moroka R, *et al.* Branched-chain amino acid supplementation reduces oxidative stress and prolongs survival in rats with advanced liver cirrhosis. *PLoS ONE* 2013; **25(8)**: e70309.

49. Muto Y, Sato S, Watanabe A, *et al.* Effects of oral branched-chain amino acid granules on event-free survival in patients with liver cirrhosis. *Clin Gastroenterol Hepatol* 2005; **3**: 705–13.

50. Ijichi C, Matsumura T, Tsuji T, Eto Y. Branched-chain amino acids promote albumin synthesis in rat primary hepatocytes through the mTOR signal transduction system. *Biochem Biophys Res Commun* 2003; **303**: 59–64.

Supporting information

Additional Supporting Information may be found in the online version of this article:

Fig. S1. Twenty five patients with HCV-related advanced fibrosis enrolled Human BCAA supplementation study. Advanced fibrosis defined liver specimens (METAVIR fibrosis staging: >F3,4) or Fib-4 index (>3.25).

Fig. S2. HDAC activity of HCV TgM fed the excess-iron diet with BCAA was significantly lower than those of HCVTgM fed the excess-iron diet with casein or the control diet. All samples were nuclear which was extracted from liver tissue.

JSGE 1898 The Japanese Society of Gastroenterology

ORIGINAL ARTICLE—LIVER, PANCREAS, AND BILIARY TRACT

Association between *Wisteria floribunda* agglutinin-positive Mac-2 binding protein and the fibrosis stage of non-alcoholic fatty liver disease

Masanori Abe · Teruki Miyake · Atsushi Kuno · Yasuharu Imai ·
Yoshiyuki Sawai · Keisuke Hino · Yuichi Hara · Shuhei Hige · Michiie Sakamoto ·
Gotaro Yamada · Masayoshi Kage · Masaaki Korenaga · Yoichi Hiasa ·
Masashi Mizokami · Hisashi Narimatsu

Abstract

Background Accurately evaluating liver fibrosis in patients with non-alcoholic fatty liver disease (NAFLD) is important for identifying those who may develop complications. The aims of this study were (1) to measure serum *Wisteria floribunda* agglutinin-positive Mac-2 binding protein (WFA$^+$-M2BP) using the glycan sugar chain-based immunoassay and (2) to compare the results with clinical assessments of fibrosis.

Methods Serum WFA$^+$-M2BP values were retrospectively evaluated in 289 patients with NAFLD who had undergone liver biopsy. Histological findings were evaluated by three blinded, experienced liver-specific pathologists.

Results For stages 0 ($n = 35$), 1 ($n = 113$), 2 ($n = 49$), 3 ($n = 41$), and 4 ($n = 51$) of liver fibrosis, the serum WFA$^+$-M2BP cutoff indexes were 0.57, 0.70, 1.02, 1.57, and 2.96, respectively. Multivariate regression analysis showed that serum WFA$^+$-M2BP values were associated with the stage of fibrosis ($\geq$stage 2). The areas under the receiver operating characteristic curve (AUROC), sensitivity, and specificity of serum WFA$^+$-M2BP were 0.876, 85.9, and 74.6 %, respectively, for severe fibrosis ($\geq$stage 3) and were 0.879, 74.6, and 87.0 %, respectively, for cirrhosis. When compared with six non-invasive conven-

M. Abe (✉) · T. Miyake · Y. Hiasa
Department of Gastroenterology and Metabology, Ehime
University Graduate School of Medicine, Toon,
Ehime 791-0295, Japan
e-mail: masaben@m.ehime-u.ac.jp

M. Abe · T. Miyake · A. Kuno · Y. Imai · Y. Sawai ·
K. Hino · Y. Hara · S. Hige · M. Sakamoto · M. Korenaga ·
M. Mizokami · H. Narimatsu
The Hepatitis Glyco-biomarker Study Group, Tokyo, Japan

A. Kuno · H. Narimatsu
Research Center for Medical Glycoscience, National Institute of
Advanced Industrial Science and Technology, Tsukuba, Ibaraki,
Japan

Y. Imai · Y. Sawai
Department of Gastroenterology, Ikeda Municipal Hospital,
Ikeda, Osaka, Japan

K. Hino · Y. Hara
Department of Hepatology and Pancreatology, Kawasaki
Medical School, Kurashiki, Okayama, Japan

S. Hige
Department of Hepatology, Sapporo-Kosei General Hospital,
Sapporo, Hokkaido, Japan

M. Sakamoto
Department of Pathology, Keio University School of Medicine,
Tokyo, Japan

G. Yamada
Department of General Internal Medicine 2, Kawasaki Medical
School, Kurashiki, Okayama, Japan

M. Kage
Department of Diagnostic Pathology, Kurume University
Hospital, Kurume, Fukuoka, Japan

M. Korenaga · M. Mizokami
The Research Center for Hepatitis and Immunology, National
Center for Global Health and Medicine, Ichikawa, Chiba, Japan

🖄 Springer

tional markers, serum WFA$^+$-M2BP had the greatest AUROC for diagnosing severe fibrosis and cirrhosis.

Conclusions Serum WFA$^+$-M2BP values are useful for assessing the stage of liver fibrosis in patients with NAFLD.

Keywords Mac-2 binding protein · Glycoprotein · Non-alcoholic fatty liver disease · Fibrosis marker · Cirrhosis

Introduction

Non-alcoholic fatty liver disease (NAFLD) is one of the most common liver diseases worldwide and is recognized as the hepatic manifestation of metabolic syndrome [1–3]. NAFLD can be classified as simple steatosis or non-alcoholic steatohepatitis (NASH), a progressive form of chronic liver disease (CLD), resulting in cirrhosis, hepatic failure, and hepatocellular carcinoma. Accurately evaluating liver fibrosis in NAFLD patients is important for identifying those who may progress to severe clinical conditions such as liver cirrhosis and hepatocellular carcinoma [4–7]. Liver biopsies are the gold standard for diagnosing NASH and associated liver fibrosis [8]. However, there is controversy surrounding the active use of liver biopsies for these purposes, because they have several drawbacks [9, 10]. A liver biopsy is highly costly and invasive with rare but potentially life-threatening complications [11]. In addition, sampling errors may occur, because a standard liver biopsy sample represents only 1/50,000 of the whole liver [12]. Furthermore, inter- and intra-observer variability also poses serious problems for the pathological diagnosis of NAFLD [13–17]. Accordingly, there is an urgent need for a non-invasive method for estimating the stage of liver fibrosis in NA-FLD patients. Several methods using serum markers [18, 19], scoring systems [20–23], and imaging techniques, such as transient elastography [24–26], have been developed. Although each method has been reported as useful, few have been independently validated. Several problems also remain unaddressed, such as the methods' complexities, reproducibilities, and costs for routine clinical use.

Recently, we developed a new glyco-marker for liver fibrosis using the glycan sugar chain-based immunoassay. The FastLec-Hepa system was used to determine the serum values of sweet-doughnut hyperglycosylated *Wisteria floribunda* agglutinin-positive Mac-2 binding protein (WFA$^+$-M2BP) for the assessment of liver fibrosis [27–29]. Toshima et al. [30] and Yamasaki et al. [31] reported that this assay offered a feasible means of assessing liver fibrosis in patients with CLD due to the hepatitis C virus (HCV). However, the

progressive patterns of fibrosis may differ for CLD due to HCV and CLD due to NAFLD. Indeed, liver specimens from NAFLD patients show pericellular fibrosis around the central vein in the early stages, with gradual progression to fibrosis when central veins become connected to surrounding lobules. In contrast, central vein involvement in patients with CLD due to HCV is generally preceded by portal tract damage with pathological changes to the portal vein.

We investigated the clinical usefulness of serum WFA$^+$-M2BP values in patients with well-characterized NAFLD. First, we confirmed the efficacy of serum WFA$^+$-M2BP values for assessing the stage of fibrosis. Second, we compared the diagnostic performances of serum WFA$^+$-M2BP and other non-invasive fibrosis markers and tests that are used to estimate the stage of liver fibrosis.

Methods

Patients

We retrospectively reviewed 325 NAFLD patients who underwent liver biopsy at Ehime University Hospital (Ehime, Japan), Ikeda Municipal Hospital (Osaka, Japan), Kawasaki Medical School Hospital (Okayama, Japan), or Sapporo Kosei General Hospital (Hokkaido, Japan). The exclusion criteria were as follows: a history of other liver diseases, including hepatitis B virus or HCV infection; administration of drugs that influence the activity of the disease, such as tamoxifen or a glucocorticoid; or a history of alcohol abuse (defined as ≥20 g of alcohol daily). Written informed consent was obtained from all patients who participated. The study protocol conformed to the ethical guidelines of the 1975 Declaration of Helsinki, as reflected by each institutional review committee's a priori approval of this study.

Histological evaluation

Each NAFLD patient received a liver biopsy under laparoscopy or ultrasonography between July 2003 and September 2013. The biopsied liver samples were fixed in formalin and were embedded in paraffin according to the standard procedure at each institution. Slices (4 μm thick) were stained with hematoxylin and eosin (H&E), Azan-Mallory, silver, and Elastica van Gieson at Keio University. Liver samples <15 mm long were excluded, because the detection of liver fibrosis may be affected by sampling errors with such samples. A minimum of six portal tracts in the specimen was required for diagnosis. All liver samples were independently evaluated by three experienced liver-specialized pathologists (M.S., G.Y., and M.K.) who were blinded to the clinical data, and all evaluations were validated through discussion. The liver fibrosis stages were

assessed according to Brunt's criteria [32]. Significant and severe fibrosis was defined as ≥stage 2 and ≥stage 3, respectively. Thirty-six patients were excluded because of clinical and/or histological reasons; thus, 289 patients were included in the final analysis.

Clinical and biochemical data

Relevant clinical data were recorded, including the patient's age, sex, weight, and height. Body mass index (BMI) was calculated as weight (kg) divided by height (m) squared. Venous blood samples were obtained in the morning after overnight fasting, either immediately before or no more than 2 months after liver biopsy. The blood samples were stored at −80 °C until analysis.

The biochemical variables were measured using a conventional automated analyzer at the respective hospitals. We analyzed the serum levels for the following: platelet count, prothrombin time, bilirubin, aspartate aminotransferase (AST), alanine aminotransferase (ALT), gamma-glutamyl-transpeptidase, albumin, cholesterol, triglyceride, fasting plasma glucose (FPG), ferritin, and hyaluronic acid. The AST-to-platelet ratio index (APRI) was calculated as follows: [AST (U/L)/UNL × 100]/platelet count. In this equation, UNL is the upper limit of the normal AST [33]. The FIB-4 index was calculated as follows: age (years) × AST (U/L)/platelet count ($\times 10^9$/L) × $\sqrt{\text{ALT}}$ (U/L) [20]. The NAFLD fibrosis score was calculated as follows: $-1.675 + 0.037 \times$ age (years) $+ 0.094 \times$ BMI (kg/m^2) $+ 1.13 \times$ impaired fasting glycemia or diabetes (yes $= 1$; no $= 0$) $+ 0.99 \times$ AST/ALT ratio $- 0.013 \times$ platelet ($\times 10^9$/L) $- 0.66 \times$ albumin (g/dL) [21].

Serum Wisteria floribunda agglutinin-positive Mac-2 binding protein value

The WFA$^+$-M2BP value in sera was measured by a WFA-antibody immunoassay using a chemiluminescence enzyme immunoassay machine (HISCL-2000i; Sysmex, Kobe, Japan), as previously reported [27, 28, 30, 31]. The measured values of WFA$^+$-M2BP using the conjugated WFA were indexed with the obtained values using the following equation: cutoff index (COI) = ([WFA$^+$-M2BP]$_{\text{sample}}$ − [WFA$^+$-M2BP]$_{\text{NC}}$) ÷ ([WFA$^+$-M2BP]$_{\text{PC}}$) − [WFA$^+$-M2BP]$_{\text{NC}}$). In this equation, [WFA$^+$-M2BP]$_x$ denotes the [WFA + -M2BP] count of the serum sample ($x = $ sample), positive control ($x = $ PC), or negative control ($x = $ NC).

Statistical analysis

Quantitative values are presented as mean ± standard deviation, unless otherwise noted. The Steel–Dwass test was used for multiple comparisons of continuous variables among the different groups. Univariate and multivariate analyses were performed using a logistic regression model. Each cutoff value was determined from the receiver operating characteristic (ROC) curve analyses. The diagnostic performances of the markers were expressed as the diagnostic specificity, sensitivity, positive predictive value, negative predictive value, and area under the ROC (AUROC) curve. p values <0.05 were considered statistically significant. All statistical analyses were performed using JMP, version 11 software (SAS Institute, Tokyo, Japan).

Results

Cross-sectional association between Wisteria floribunda agglutinin-positive Mac-2 binding protein values and the fibrosis stage

The patients' characteristics are summarized in Table 1. The mean age of the 289 patients (159 men and 130 women) was 54.8 ± 14.6 years old. Figure 1 shows the serum WFA$^+$-M2BP values for each fibrosis stage. The serum WFA$^+$-M2BP values measured by glycan-based immunoassay ranged from 0.12 to 11.06 (COI). The

Table 1 Patients' clinical characteristics and laboratory data

Features	Total ($n = 289$)
Male/female	159/130
Age (years)	54.8 ± 14.6
Body mass index (kg/m^2)	27.6 ± 4.7
Platelet count (10^9/l)	18.9 ± 6.8
Prothrombin time (%)	99.3 ± 16.7
Bilirubin (mg/dl)	0.97 ± 0.6
AST (U/l)	61.4 ± 48.9
ALT (U/l)	85.5 ± 68.9
GGT (U/l)	92.3 ± 89.9
Albumin (g/dl)	4.2 ± 0.4
Cholesterol (mg/dl)	195.4 ± 41.1
Triglyceride (mg/dl)	144.4 ± 77.2
FPG (mg/dl)	115.2 ± 38.4
Ferritin (ng/ml)	261.2 ± 258.5
WFA$^+$-M2BP (COI)	1.26 ± 1.44
Fibrosis stage (0/1/2/3/4)	35/113/49/41/51

Values are expressed as mean ± standard deviation

AST aspartate aminotransferase, ALT alanine aminotransferase, COI cutoff index, GGT gamma-glutamyl transpeptidase, FPG fasting plasma glucose, WFA$^+$-M2BP Wisteria floribunda agglutinin-positive Mac-2 binding protein

Fig. 1 The serum *Wisteria floribunda* agglutinin-positive Mac-2 binding protein (WFA$^+$-M2BP) values for each fibrosis stage. The *top* and *bottom* of each *box* represent the first and third quartiles, respectively, with the height of the box representing the interquartile range, covering 50 % of the values. The *line* across each *box* represents the median. The *whiskers* show the highest and lowest values. All pairs of groups are significantly different, as assessed using the Steel–Dwass test ($p < 0.01$). *COI* cutoff index
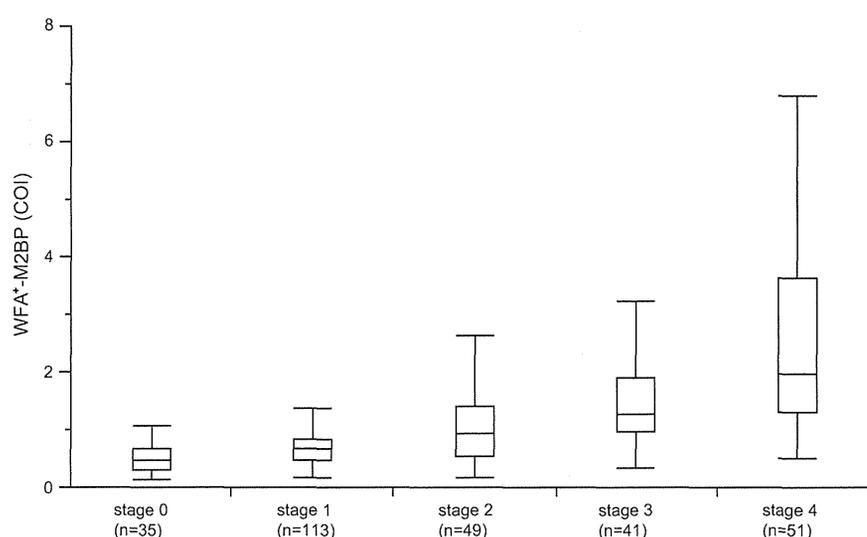
Table 2 Variables associated with the fibrosis stage according to multivariate regression analyses

	Stage 0 vs. stages 1–4		Stages 0–1 vs. stages 2–4		Stages 0–2 vs. stages 3–4		Stages 0–3 vs. stage 4	
	Odds ratio (95 % CI)	p value	Odds ratio (95 % CI)	p value	Odds ratio (95 % CI)	p value	Odds ratio (95 % CI)	p value
Age (years)			1.049 (1.014–1.087)	0.006				
BMI (kg/m^2)	1.228 (1.089–1.412)	0.002						
Platelet count (10^9/L)					0.864 (0.787–0.941)	0.001	0.895 (0.814–0.978)	0.017
Prothrombin time (%)	0.948 (0.914–0.982)	0.004	0.957 (0.925–0.986)	0.007			0.963 (0.927–0.993)	0.028
AST (U/l)	1.078 (1.023–1.144)	0.008	1.036 (1.022–1.052)	<0.001				
FPG (mg/dl)			1.013 (1.004–1.024)	0.007	1.014 (1.004–1.024)	0.004	1.012 (1.002–1.022)	0.013
WFA$^+$-M2BP (COI)			5.875 (2.339–16.369)	<0.001	8.471 (3.562–22.725)	<0.001	2.390 (1.463–4.423)	0.002

CI confidence interval, *BMI* body mass index, *AST* aspartate aminotransferase, *FPG* fasting plasma glucose, WFA$^+$-*M2BP Wisteria floribunda* agglutinin-positive Mac-2 binding protein, *COI* cutoff index

WFA$^+$-M2BP value in patients with stages 0 ($n = 35$), 1 ($n = 113$), 2 ($n = 49$), 3 ($n = 41$), and 4 ($n = 51$) of fibrosis had COIs of 0.57, 0.70, 1.02, 1.57, and 2.96, respectively, demonstrating a stepwise increase with an increasing severity of liver fibrosis (Fig. 1). All pairs of groups differed significantly according to the Steel–Dwass test (stage 0 vs. stage 1, $p = 0.012$; stage 0 vs. stage 2, $p < 0.001$; stage 0 vs. stage 3, $p < 0.001$; stage 0 vs. stage 4, $p < 0.001$; stage 1 vs. stage 2, $p = 0.002$; stage 1 vs. stage 3, $p < 0.001$; stage 1 vs. stage 4, $p < 0.001$; stage 2 vs. stage 3, $p = 0.014$; stage 2 vs. stage 4, $p < 0.001$; and stage 3 vs. stage 4, $p = 0.008$).

Comparisons of variables associated with the diagnosis of the fibrosis stage

The variables associated with each stage of liver fibrosis were assessed by univariate and multivariate analyses (Tables S1, 2).

Variables associated with the presence of fibrosis (≥stage 1)

According to univariate analysis, eight variables (age, BMI, platelet count, prothrombin time, AST, ALT,

albumin, and the WFA$^+$-M2BP value) were associated with the presence of fibrosis (Table S1). Multivariate analysis showed that the BMI [odds ratio (OR) 1.228, 95 % confidence interval (CI) 1.089–1.412], prothrombin time (OR 0.948; 95 % CI 0.914–0.982), and AST (OR 1.078; 95 % CI 1.023–1.144) were independently associated with the presence of fibrosis (Table 2).

Variables associated with the presence of significant fibrosis (≥stage 2)

Univariate analysis identified ten variables (sex, age, platelet count, prothrombin time, bilirubin, AST, albumin, cholesterol, FPG, and the WFA$^+$-M2BP value) that were associated with the presence of significant fibrosis (Table S1). However, multivariate analysis showed that age (OR 1.049; 95 % CI 1.014–1.087), prothrombin time (OR 0.957; 95 % CI 0.925–0.986), AST (OR 1.036; 95 % CI 1.022–1.052), ALT (OR 1.036; 95 % CI 1.022–1.052), FPG (OR 1.013; 95 % CI 1.004–1.024), and the WFA$^+$-M2BP value (OR 5.875; 95 % CI 2.339–16.369) were independently associated with the presence of significant fibrosis (Table 2).

Variables associated with the presence of severe fibrosis (≥stage 3)

According to univariate analysis, ten variables (sex, age, platelet count, prothrombin time, bilirubin, albumin, cholesterol, triglyceride, FPG, and the WFA$^+$-M2BP value) were associated with the presence of severe fibrosis (Table S1). However, multivariate analysis showed that the platelet count (OR 0.864; 95 % CI 0.787–0.941), FPG (OR 1.014; 95 % CI 1.004–1.024), and the WFA$^+$-M2BP value (OR 8.471; 95 % CI 3.562–22.725) were independently associated with the presence of severe fibrosis (Table 2).

Variables associated with the presence of cirrhosis (stage 4)

Univariate analysis identified 11 variables (sex, age, platelet count, prothrombin time, bilirubin, ALT, albumin, cholesterol, triglyceride, FPG, and the WFA$^+$-M2BP value) that were associated with the presence of cirrhosis (Table S1). Multivariate analysis identified that the platelet count (OR 0.895; 95 % CI 0.814–0.978), prothrombin time (OR 0.963; 95 % CI 0.927–0.993), FPG (OR 1.012; 95 % CI 1.002–1.022), and the WFA$^+$-M2BP value (OR 2.390; 95 % CI 1.462–4.423) were independently associated with the presence of cirrhosis (Table 2).

Diagnostic power of the *Wisteria floribunda* agglutinin-positive Mac-2 binding protein values for each fibrosis stage

The WFA$^+$-M2BP ROC curves for diagnosing each fibrosis stage are presented in Fig. 2. The AUROC curve values (95 % CI) for the prediction of ≥stage 1, ≥stage 2, ≥stage 3, and stage 4 using the serum WFA$^+$-M2BP values were 0.788 (0.736–0.833), 0.838 (0.790–0.879), 0.876 (0.832–0.911), and 0.879 (0.835–0.914), respectively (Table 3). The optimal cutoff values were 0.59 for ≥stage 1, 0.90 for ≥stage 2, 0.94 for ≥stage 3, and 1.46 for stage 4 (Table 3). The sensitivities for the prediction of ≥stage 1, ≥stage 2, ≥stage 3, and stage 4 were 74.8, 77.3, 85.9, and 72.6 %, respectively; whereas, the specificities were 74.3, 81.1, 74.6, and 87.0 %, respectively (Table 3).

Comparisons of AUROC curve values for diagnosing the fibrosis stage

The AUROC curve values for diagnosing each fibrosis stage are shown in Table 4. Compared with the other surrogate markers and scoring systems, the serum WFA$^+$-M2BP was the most useful marker for differentiating stages 0–2 from stages 3–4 and stages 0–3 from stage 4. The AUROC curve values for differentiating stages 0–1 from stages 2–4 were compatible with the serum WFA$^+$-M2BP (0.838), hyaluronic acid (0.833), and the FIB-4 index (0.844).

Discussion

Clinically, it is very important to identify patients who have NASH with advanced fibrosis, because these patients have more liver-related complications and a greater mortality rate than patients who have NASH without liver fibrosis [4–7]. Although a liver biopsy is the gold standard for diagnosing and assessing the stages of fibrosis, research on noninvasive methods for assessing the fibrosis stages have rapidly evolved over the last decade [17–26]. In this study, we found that the serum WFA$^+$-M2BP values measured using a glycan-based immunoassay provided a useful diagnostic factor for assessing the liver fibrosis stage in NAFLD patients (Fig. 1). The glycan-based immunoassay was previously developed as a simple system for automatically detecting unique fibrosis-related glycoalterations [27–31]. Moreover, the accuracy of the serum WFA$^+$-M2BP values for diagnosing severe fibrosis and cirrhosis was superior to that offered by other surrogate markers and tests (Table 4).

M2BP is a secreted glycoprotein that is found in the serum of healthy individuals, but its concentration
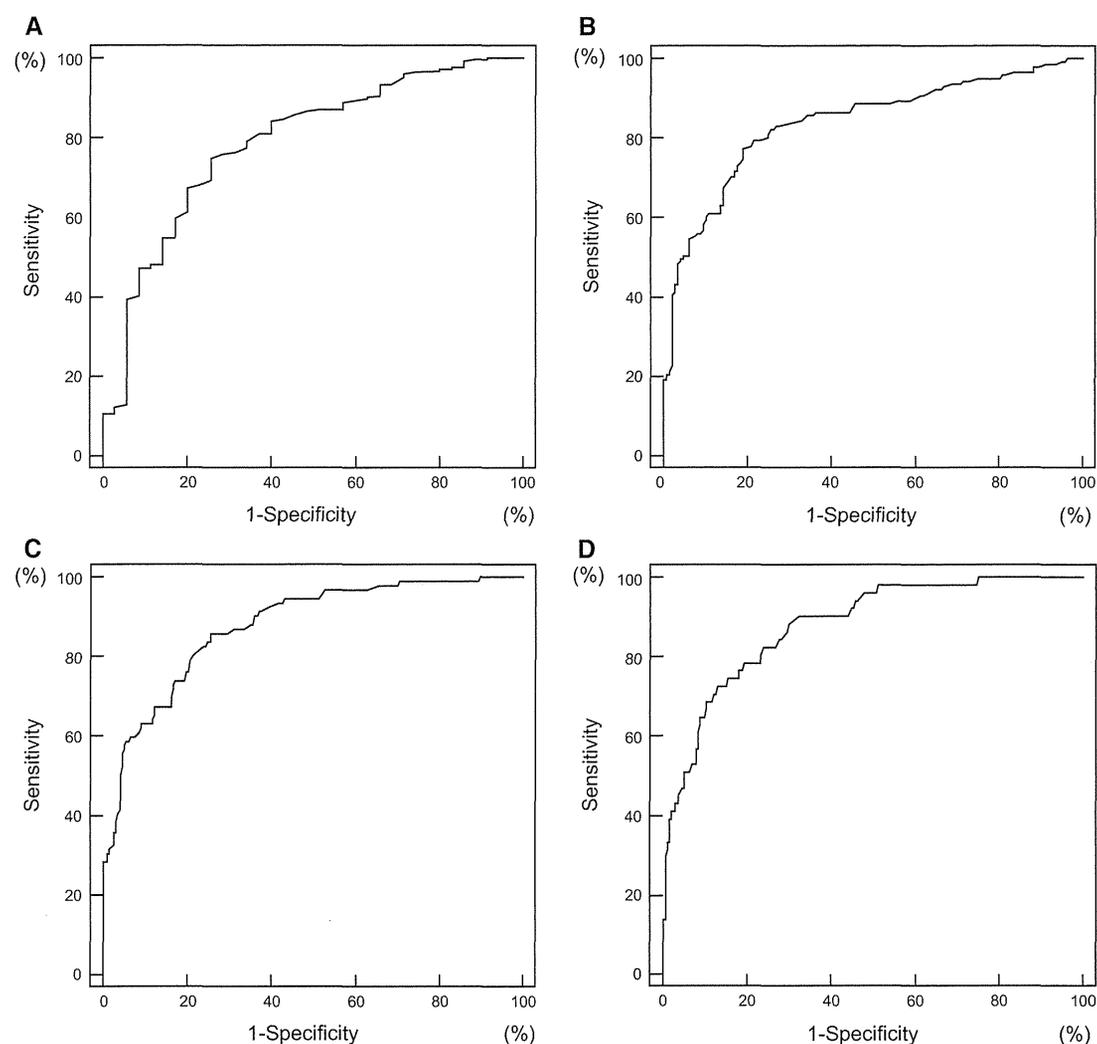
Fig. 2 The diagnostic capabilities of the serum *Wisteria floribunda* agglutinin-positive Mac-2 binding protein (WFA$^+$-M2BP) values for assessing the stage of liver fibrosis. The areas under the receiver operating characteristic curve of serum WFA$^+$-M2BP for diagnosing liver fibrosis were as follows: **a** 0.788 for stage $\geq$1; **b** 0.838 for stage $\geq$2; **c** 0.876 for stage $\geq$3; and **d** 0.879 for stage 4

increases in patients with various cancers and viral infections, including HCV [34, 35]. This protein binds galectin-3, β-1 integrins, collagens, and fibronectin and has some relevance to cell–cell and cell–extracellular matrix adhesion [36, 37]. Therefore, it is reasonable to assume that M2BP reflects the progression of fibrosis in cases of CLD. Indeed, using proteome analysis, Cheung et al. [38] found that serum M2BP is a potential marker of fibrosis progression in HCV patients.

In this study, we found that the serum WFA$^+$-M2BP value can be used to distinguish the fibrosis stages in NAFLD patients (Fig. 1; Tables S1, 2, 3). Recently, Kamada et al. [39] reported that the serum M2BP value (the whole M2BP protein measured by enzyme-linked immunosorbent assay) can be used for predicting the fibrosis

stage in NAFLD patients. However, there are several differences between the present study and Kamada et al.'s study. In our study, the serum WFA$^+$-M2BP value (the altered M2BP with fibrosis-related *N*-glycans measured by glycan-based immunoassay) increased stepwise with the increasing severity of liver fibrosis, whereas a stepwise increase was not found in Kamada et al.'s study. Further, our method can distinguish between the fibrosis stages more clearly, not only in patients with advanced fibrosis stage but also in those with earlier fibrosis stages of NA-FLD (Fig. 1). In our previous study [27], we found that both the quantity and quality of M2BP were altered during the progression of fibrosis of CLD due to HCV. Since the *N*-glycosylation of M2BP was dramatically altered during the progression of liver fibrosis, we considered that the

Table 3 Serum *Wisteria floribunda* agglutinin-positive Mac-2 binding protein values for assessing liver fibrosis

Stage	AUC (95 % CI)	Cutoff level	Sensitivity (%)	Specificity (%)	PPV (%)	NPV (%)	Predictive accuracy (%)
≥Stage 1	0.788 (0.736–0.833)	0.59	74.8	74.3	95.5	28.9	74.7
≥Stage 2	0.838 (0.790–0.879)	0.90	77.3	81.1	79.6	78.9	79.2
≥Stage 3	0.876 (0.832–0.911)	0.94	85.9	74.6	61.2	91.9	78.2
Stage 4	0.879 (0.835–0.914)	1.46	72.6	87.0	54.4	93.7	84.4

AUC area under receiver operating characteristic curve, *CI* confidence interval, *PPV* positive predictive value, *NPV* negative predictive value

Table 4 Comparisons of the areas under the receiver operating characteristic curves for each fibrosis marker and scoring system

Marker and score	≥Stage 1	≥Stage 2	≥Stage 3	Stage 4
WFA+-M2BP	0.788	0.838	0.876	0.879
Platelet count	0.649	0.719	0.810	0.815
Hyaluronic acid	0.757	0.833	0.856	0.858
AST/ALT ratio	0.607	0.733	0.770	0.752
APRI	0.867	0.804	0.758	0.745
FIB-4 index	0.793	0.844	0.857	0.849
NAFLD fibrosis score	0.766	0.811	0.808	0.824

WFA+-*M2BP Wisteria floribunda* agglutinin-positive Mac-2 binding protein, *AST* aspartate aminotransferase, *ALT* alanine aminotransferase, *APRI* AST-to-platelet ratio index, *NAFLD* non-alcoholic fatty liver disease

WFA+-M2BP reflects the fibrosis status more precisely than the whole M2BP protein. Further, the quantification of the WFA+-M2BP may offer a better marker for assessing the liver fibrosis stage than does the quantification of the M2BP protein. Currently, the N-glycan structures of WFA−-M2BP and WFA+-M2BP are being analyzed using mass spectrometry in our laboratory. Moreover, our system has been converted to a fully automated immunoassay analyzer for clinical use, featuring a measurement time of only 17 min, which has clear practical implications [27, 28, 30, 31].

Numerous non-invasive panels of the tests have been developed to assess the liver fibrosis stages [17–26]. In this study, the serum WFA+-M2BP values offered a superior AUROC curve for the diagnosis of severe fibrosis and cirrhosis compared with the FIB-4 index and five other markers and scoring systems (Table 4). In a study of a large Japanese cohort, the FIB-4 index was the most useful index for diagnosing patients with advanced fibrosis [40]. Although the American Association for the Study Liver Diseases' guidelines [3] recommend the NAFLD fibrosis score [21] when deciding whether to perform a liver biopsy, the usefulness of this score remains questionable in

Asian patients [40, 41]. Consistent with these studies, the NAFLD fibrosis score yielded lower AUROCs than the WFA+-M2BP values and the FIB-4 index for diagnosing fibrosis in our cohort (Table 4).

There are two main strengths of the present study's cohort. First, the sample size ($n = 289$) was relatively large, and the patients' clinical backgrounds were well characterized. Second, the pathological diagnoses were performed and validated by three experienced liver-specific pathologists. Currently, the definitive diagnosis of NAFLD and the distinction of its phenotypes rely on the pathologist's interpretation of the liver biopsy [8]; therefore, an accurate and reproducible consensus regarding the pathological findings is necessary for diagnosing NAFLD. However, in practice, the interpretation of NAFLD's histology varies substantially. In this study, we excluded patients whose liver samples were inadequate for histological evaluation (e.g., because of insufficient sample size). Moreover, the considerable rate of inter-observer variation is one of the major problems in the histological diagnosis of NAFLD [13–17]. Our strategy mainly focused on reducing this variation, and our study may provide a reliable cohort for identifying surrogate markers and for investigating the management of NAFLD patients.

This study also has several limitations. First, we investigated the usefulness of the serum WFA+-M2BP values in a cross-sectional study. Therefore, the use of the serum WFA+-M2BP values for monitoring natural history, predicting outcomes, and predicting responses to therapeutic interventions remain unknown. In fact, the prevalence of NAFLD is high among individuals with diabetes or dyslipidemia [1–3], and some patients have already managed their condition through lifestyle interventions and/or medication at the time of liver biopsy. Further prospective studies are necessary to address these issues. In addition, since the biochemical analyses were performed separately at the respective hospitals, any variations among each institution cannot be ruled out. Moreover, several selection